ELSEVIER

Marine Structures 15 (2002) 211–231

MARINE STRUCTURES

www.elsevier.com/locate/marstruc

Risk assessment of aging ship hull structures in the presence of corrosion and fatigue

Unyime O. Akpan[a,*], T.S. Koko[a], B. Ayyub[b], T.E. Dunbar[a]

[a] *Department of Research and Emerging Technologies, Martec Limited, Suite 400, 1888 Brunswick Street, Halifax, Nova Scotia, Canada B3J 3J8*

[b] *BMA Engineering Inc., 11429 Palatine Drive, Potoma, MA, USA*

Received 17 July 2001; accepted 5 November 2001

Abstract

An approach for risk assessment of the ultimate strength of an aging ship hull structure that is being degraded by corrosion and fatigue is developed. Time-dependent random function models for corrosion growth, fatigue cracks and corrosion-enhanced fatigue cracks that weaken the capacity of a ship hull are presented. The second-order reliability method is used to calculate instantaneous reliability of the primary hull structure. Methodology for computing the time-dependent reliability of a degrading aging ship structure is developed. Sensitivity of aging structure reliability to statistical and probabilistic description of corrosion and fatigue crack parameters is investigated. An example of a problem involving an aging tanker structure is used for demonstration. © 2002 Published by Elsevier Science Ltd.

Keywords: Risk; Time-dependent reliability; Fatigue; Corrosion; Aging; Hull-structure; Degradation

1. Introduction

Corrosion and fatigue cracking are the most pervasive types of structural problems experienced by ship structures. Each of the damage modes, if not properly monitored and rectified, can potentially lead to catastrophic failure or unanticipated out-of-service time. These problems are a major threat to the structural integrity of aging vessels, especially tanker structures and bulk carriers, many of which continue to operate beyond their design service life. The importance of monitoring and mitigating corrosion and fatigue has been recognized by classification societies, ship

*Corresponding author. Tel.: +1-902-425-5101; fax: +1-902-425-1923.

E-mail address: uakpan@martec.com (U.O. Akpan).

0951-8339/02/$ - see front matter © 2002 Published by Elsevier Science Ltd.

PII: S0951-8339(01)00030-2

owners and International Maritime Organizations. Standards for accessing the structural integrity of aging vessels are being developed by the various agencies. For example, the Tanker Structure Cooperative Forum (TSCF) has issued extensive guidelines for aging and corroding vessels. TSCF has issued typical deterministic corrosion rates for uncoated steel of longitudinal primary members in cargo oil tankers. Minimal allowable sizes for the different components have also been issued by various classification societies. Bea et al. [1] conducted extensive research on the significance of fatigue crack and corrosion in tankers. However, there are very few studies that model the impact of corrosion and fatigue cracking on the structural integrity of the ship hull structure [2].

Modeling the impact of corrosion and fatigue cracking on the structural integrity of a ship hull is complicated by the high level of uncertainties associated with these modes of failure. The occurrence of corrosion and fatigue cracks, their spatial distribution on a structure, and the time-dependent growth and interactions in-service are random phenomena, therefore probabilistic models must be employed in analyzing their effect.

The present study is focused on assessing the effect of corrosion and fatigue crack on the structural integrity of a ship hull structure. The strength of a ship hull is modeled as a random process that decreases in the presence of corrosion and fatigue cracks. Corrosion and fatigue crack growth rates at the various longitudinal section members are modeled as random variables. Extreme loads that are applied at random times to the hull structure are modeled. Second-order reliability analysis methodology (SORM) is used to compute instantaneous reliability. Hazard rate function is defined and used in the estimation of time-variant reliability of a corroded cracked ship structure. An aging tanker example is used for demonstration. The effect of corrosion growth rate, initial crack sizes and interactions between cracks and corrosion on the time-dependent structural integrity of the vessel is studied.

2. Ultimate strength limit state

Assessing the structural risk of a degrading vessel requires the development of an ultimate strength limit-state function with reference to the primary ship hull structure. Reference is usually made to the midship section. The ship hull is considered to behave globally as a beam under transverse load subjected to still-water and wave-induced effects. The governing limit-state model for the ultimate strength can be defined by

$$g(t) = U(t) - M_L(t), \tag{1}$$

where $U(t)$ is a model of the ultimate strength capacity of the vessel and $M_L(t)$ is a model of the effect of external load on the vessel. Degradation of the primary ship structure results in a time-varying decreasing ultimate strength capacity. Eq. (1) can be defined in terms of the vertical bending moment that induces bending of the hull. For the ultimate collapse of a hull girder, the underlying random functions can be defined as

$$U(t) = M_u(t) \quad (2)$$

and

$$M_L(t) = M_{sw}(t) + k_w(M_w(t) + k_D M_{Dyn}(t)), \quad (3)$$

where $M_u(t)$ is the ultimate hull girder bending moment capacity, M_{sw} is the still-water bending moment, M_w is the wave-induced bending moment, M_{Dyn} is the dynamic bending moment, and k_{Dyn} is the correlation factor between wave-induced and dynamic bending moments. The correlation factor, k_{Dyn}, depends on whether the bending is of the hogging type or sagging type [3–5]. For simplicity, the simple linear model, $M_L(t) = M_{sw}(t) + M_w(t)$ employed by Mansour and Thayamballi (1994) will be used in the illustrative example problem. Furthermore, $M_{sw}(t)$ and $M_w(t)$ can be functions of time. However, in this study, they are assumed to be independent of time in order to simplify the demonstration of the suggested methodology.

2.1. Ultimate hull girder bending moment capacity

Various formulations for estimating the ultimate hull girder bending moment capacity, $M_u(t)$, of ship structures have been developed. They range from simple analytical to complicated numerical models. A review of the methods, their advantages and limitations are given in Mansour et al. [6] and Thayamballi et al. [7]. These formulations have the following characteristics:

(i) ultimate strength obtained by applying a buckling knockdown factor to the hull girder fully plastic bending moment [8,9];
(ii) ultimate strength obtained by reduced elastic section modulus accounting for plate buckling at deck and bottom [10];
(iii) ultimate strength obtained by longitudinal stiffened single cell rectangular construction; compression flange treated by a beam-column idealization [11];
(iv) ultimate strength based on load and end-shortening curves for beam column and tripping failure; aimed at longitudinally stiffened vessel [12];
(v) ultimate strength based on load and end-shortening curves; hard spots subjectively treated; elasto-plastic *FEM* for load and end-shortening curves of plate–stiffener combinations [13]; and
(vi) ultimate strength based on dynamic non-linear elasto-plastic finite element analysis of a large portion of the hull using beam elements and isotropic and orthotropic plate elements [14].

Computer programs for computing ultimate strength capacities, for example ALPS/ISUM [15], have been developed. The formula given in Mansour and Howen [9], is used in the current study. The hull girder bending moment capacity is estimated by

$$M_u(t) = \phi\sigma_u Z(t), \quad (4)$$

where ϕ is a non-dimensional factor known as buckling knock down factor; σ_u is the ultimate strength of the ship hull crosssection; $Z(t)$ is the midship hull elastic section modulus. In cases where a relationship between damage, such as fatigue crack and corrosion, and σ_u can be established, σ_u should be replaced with that relationship. It is well known that structural degradations will affect the hull girder capacity by reducing the section modulus $Z(t)$ with time. The impact of the degradation mechanisms and the modeling strategies that are adopted herein are presented in the following sections. The buckling knock down factor is of high variability and depends on the ship type or class and the location of a section, i.e., station.

2.2. Modeling the effect of general corrosion

Corrosion reduces the section modulus of the hull of a ship structure by thinning the thickness of primary structural members. It reduces the ability of the structure to resist the externally induced bending moment. Several models of general corrosion growth have been suggested [16–19]. The most commonly used model is

$$r(t) = C_1(t - t_0)^{C_2}, \tag{5}$$

where $r(t)$ is the thickness reduction; t_0 is the life of coating (years); t is the age of the vessel (years); C_1, C_2 are random variable coefficients; C_1 represents annual corrosion rate and although C_2 can take values ranging from 1/3 to 1, a value of 1 is used in the example problem. The life of coating varies for different vessels and depends on the coating type. Thus, in the presence of corrosion, the moment capacity is given by

$$M_u(t) = \phi\sigma_u \begin{cases} Z(r(t_0)), & t \leqslant t_0, \quad r(t_0) = 0, \\ Z(r(t)), & t > t_0, \quad r(t) > 0. \end{cases} \tag{6}$$

Formula for calculating midship section modulus $Z(r(t))$ can be found in any standard monograph on ship structures such as Hughes [20].

2.3. Modeling the effect of fatigue cracks

The presence of a fatigue crack can lead to loss of effectiveness of a structural element when the crack reaches a critical size. Thus, the net section modulus that resists longitudinal loads is reduced. The reduction may be in such a way as to increase the nominal stress levels within amidship, which in turn increases the rate of crack growth. The two main approaches for assessing fatigue strength are:

(i) S–N for crack-initiation assessment, and
(ii) fracture mechanics for crack-propagation assessment.

The S–N approach predicts the strength based on crack initiation of a critical structural detail as a function of the number of stress cycles. The fracture mechanics approach can be used in risk analysis based on crack-propagation assessment.

The fracture mechanics approach uses crack-growth equations to predict the size of a crack as a function of time. Two formulations for predicting the size of a crack, namely, mechanistic and non-mechanistic have been reported (Yang and Manning, 1990). The mechanistic model relates the crack growth to the stress intensity factor, stress range, material and environmental properties. Implementation of a mechanistic model requires a detailed knowledge of all the factors that affect crack growth. The most commonly used mechanistic model is the Paris–Erdegen formula given by

$$\frac{\mathrm{d}a}{\mathrm{d}N} = C\,\Delta K^{m}, \tag{7}$$

$$\Delta K = \Delta\sigma\; Y(a)\,\sqrt{\pi a}, \tag{8}$$

where a is the crack size; N is the number of load cycles; $\Delta\sigma$ is the stress range; ΔK is the stress intensity factor; and $Y(a)$ is a geometric factor. Assuming that $Y(a) = Y$ is a constant, the integration of Eq. (8) gives

$$a(N) = \left[a_0^{1-m/2} + \left(1 - \frac{m}{2}\right) C\,\Delta\sigma^{m}\; Y^{m}\pi^{m/2} N\right], \quad m \neq 2, \tag{9}$$

$$a(N) = a_0 \exp(C\,\Delta\sigma^{2}\; Y^{2}\pi N], \quad m = 2, \tag{10}$$

where a_o is the initial crack size; m and C are constants. In order to use Eqs. (9) and (10) for analysis, the stress range at the various details and joints must be known and practical estimation of these quantities could be very difficult. Most of the reported studies on fatigue of ship structural details have used the S–N approach. A previous study by Dobson et al. [35] used measured load spectra to calibrate the fatigue crack growth parameters, C and m for two steel materials, HY-80 and CS. The study suggested that the crack length after N load cycles can be expressed by

$$a(N) = a_0 + \sum_{i=1}^{N} \frac{\mathrm{d}a}{\mathrm{d}N}, \quad \frac{\mathrm{d}a}{\mathrm{d}N} = C\,\Delta K^{m}. \tag{11}$$

The study also showed that $C = 1.77 \times 10^{-9}$, $m = 2.54$ for HY-80 and $C = 2.54\times 10^{-9}$, $m = 2.53$ for CS material. Threshold values of stress intensity factor ΔK needed for crack growth was set at $5-6ksi/\sqrt{in}$ in the study. In order to use Eq. (11), the stress intensity factors at critical structural details have to be estimated and this is not a trivial task.

A non-mechanistic model for crack growth that can be calibrated from measured cracks and that has found wide application in the aerospace industry [36] is

$$\frac{\mathrm{d}a}{\mathrm{d}t} = Q[a(t)]^{b}, \tag{12}$$

where b and Q are crack growth parameters. Integration of Eq. (11) gives the crack size as

$$a(t) = \begin{cases} [\exp(tQ) + In(a_0)], & b = 1, \\ [tQ(1-b) + a_0^{1-b}]^{1-b}, & b \neq 1. \end{cases} \tag{13}$$

Eq. (13) can be applied to an existing ship structure with measured crack sizes at critical joints and details. The crack growth parameters a_0, b and Q can be calibrated for each critical detail. The advantage of using Eq. (12) is that it circumvents the need to mechanically model the complex mechanism of crack growth (i.e., Eqs. (9) and (11)) especially at critical structural details where the knowledge of the stress intensity factor under complex loading is not well understood. Since a database to calibrate Q, b, and a_0 might not exist for the current ship structure, Eq. (9) is used to demonstrate the risk assessment procedure. In the presence of a fatigue crack, a corrosion-enhanced fatigue crack-growth model can be given by [21]

$$a(N) = \left[a_0^{1-m/2} + \left(1 - \frac{m}{2}\right) C_{corr} C\, \Delta\sigma^m\, Y^m \pi^{m/2} N\right], \quad m \neq 2, \tag{14}$$

$$a(N) = a_0 \exp(C_{corr} C\, \Delta\sigma^2\, Y^2 \pi N], \quad m = 2 \tag{15}$$

where C_{corr} is the corrosion-enhanced fatigue crack growth parameter with a value >1. The crack at a joint in the hull girder is modeled by considering two different cracks both in the stiffener and the plate at the joint. It is assumed that a crack can be initiated at the weld between the plate and the stiffener and it can propagate in each of them as shown in Fig. 1. The crack in the plate is modeled as a through-thickness crack that propagates away from the stiffener in the transverse direction decreasing the net section modulus of the plate that resists longitudinal load. The crack in the stiffener initiates on the edge connected to the weld and propagates across the stiffener decreasing its net effective area to resist longitudinal load.

The stiffener is modeled as a flat bar with height h_{s0} and thickness b_s. The variation of the net sectional area with time depends on the crack size $a(t)$ can be computed. Thus

$$h_{si}(t) = h_{s0}(t) - a(t). \tag{16}$$

The area of the stiffener i is given by

$$A_{si}(t) = b_{si} h_{si}(t). \tag{17}$$

The moment of inertia of the ith stiffener with respect to its center of gravity is given by

$$i_{oi}(t) = \frac{b_{si} h_{si}^3(t)}{12} = \frac{b_{si}(h_{s0} - a(t))^3}{12}. \tag{18}$$

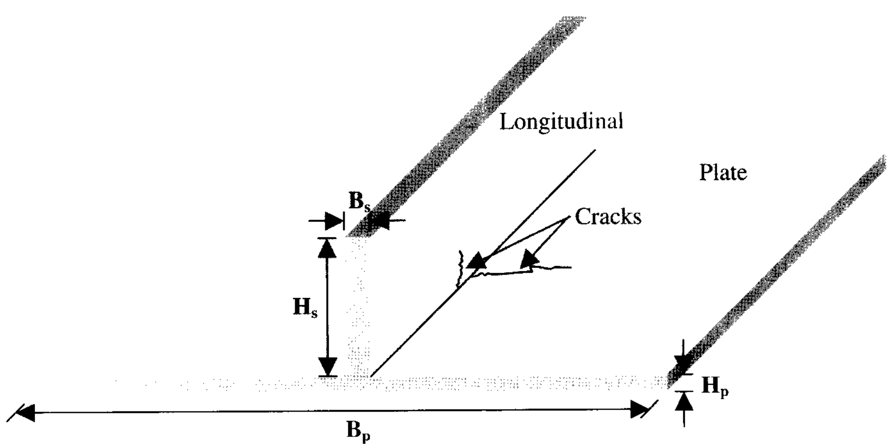

Fig. 1. Details indicating the assumed location of cracks.

Also, the plate has a breadth b_{p0} and thickness h_p. The variation of the net sectional area of the plate is given by

$$A_{pi}(t) = h_{pi}b_{pi}(t), \tag{19}$$

$$b_{pi}(t) = b_{p0}(t) - a(t) \tag{20}$$

and the moment of inertia of the ith plate element is

$$i_{oi}(t) = \frac{b_{pi}h_{pi}^3(t)}{12} = \frac{h_{pi}^3(b_{p0} - a(t))}{12}. \tag{21}$$

Eqs. (18) and (21) are used to update the section modulus of the hull girder $Z((t))$. Thus, the ultimate bending moment capacity in the presence of cracks can be written as

$$M_u(t) = \phi\sigma_u \begin{cases} Z_0, & t < t_0, \\ Z(a(t)), & t \geqslant t_0, \end{cases} \tag{22}$$

where Z_0 is the section modulus with no crack and t_0 is the time it takes for crack initiation.

2.4. Load modeling

The primary total bending moment on the hull can be decomposed into two components: the still-water bending moment M_{sw} and the wave-induced bending moment M_w. Strategies for modeling ship loads have been presented in Mansour et al. [6], where it is shown that M_{sw} and M_w are correlated. In this study, the total bending moment is calculated as the linear summation of M_{sw} and M_w.

2.4.1. Still-water bending moment (M_{sw})

The still-water bending moment is calculated from the IACS design guidance formula [22]

$$M_{sw}(t) = \begin{cases} +14.97CL^2B(8.167 - C_b)(\text{lb in}), & \text{hogging}, \\ -64.88CL^2B(0.7 + C_b)(\text{lb in}), & \text{sagging}, \end{cases} \tag{23}$$

where

$$C = \begin{cases} 2.917 \times 10^7 L, & L < 3540\,\text{in} \\ 1.559 \times 10^{-3} - \left(\dfrac{11,810 - L}{1,426,575}\right)^{1.5}, & 3540 < L < 11,810\,\text{in} \\ 1.559 \times 10^{-3}, & 11,810 < L < 13,780\,\text{in} \\ 1.559 \times 10^{-3} - \left(\dfrac{L - 13,780}{2,139,860}\right)^{1.5}, & L > 13,780\,\text{in}. \end{cases} \tag{24}$$

The above formulae are usually used to provide estimates of the deterministic design still-water bending moments for a vessel. They are thus extreme, rather than average, or point in time values, procedures for estimating point in time values of still-water bending moment will have to be developed for time-dependent reliability analysis.

2.4.2. Wave-induced bending moment (M_w)

Two general loading conditions, namely short-term and long-term conditions are used for analysis of ship structures. The long-term condition is based on adequate knowledge of the ship routes over its service life, while the short-term condition assumes that the routes are not clearly defined or can change from time to time. In short-term loading analysis, the routes that are considered the severest or the most extreme waves are used in computing the wave-induced bending moment. In the demonstration example, the short-term loading procedure is employed. A description of the short-term and long-term wave modeling strategies is given in Mansour et al. [6]. The essential steps are: identification of ship routes; computation of ocean wave statistics; calculation of extreme wave-induced bending moment using either linear or second-order strip theory [23]; and application of the largest extreme wave bending moment in analysis. For the current study, a simplified direct method based on pre-calculated seakeeping tables is used. In the proposed method developed by Loukakis and Chryssostomidis [24], seakeeping tables pre-computed based on parametric ship motion studies considering the variation in ship size, operating speed, significant wave height and block coefficient is used. Among other response parameters, the tables are designed to efficiently determine the root mean square value of the wave-induced bending moment, given the values of C_b, L/B, H_s/L, B/T, and F_n.

3. Reliability assessment strategy

The reliability of a ship structure can be defined as the likelihood of it maintaining its ability to fulfill its design purpose for some time period. In this study, the goal is to calculate both instantaneous and time-dependent reliabilities based on its ultimate strength when extreme loads act upon the vessel. The time limit state function used in the current analysis is

$$g(t) = x_u \phi \sigma_u Z(t) - x_{sw} M_{sw}(t) - x_w x_s M_s(t), \tag{25}$$

where x_u is the random variable representing modeling uncertainty in ultimate strength; x_{sw} is the random variable representing modeling uncertainty in still-water bending moment; x_w is the modeling uncertainty in wave bending moment; and x_s is a model that accounts for non-linearity in the wave bending moment. Typical values for random variables of model uncertainties are given in Mansour and Howen [9].

3.1. Instantaneous reliability

The instantaneous reliability of a ship structure may be obtained based on the limit state defined in Eq. (25), where the failure domain is defined by $\Omega = [g(t) < 0]$ and its compliment $\Omega' = [g(t) > 0]$ defines the safe domain. The instantaneous failure probability at time t is defined by

$$P_f(t) = \int_{\Omega} f(x(t))\,\mathrm{d}x, \tag{26}$$

where $f(x(t))$ is the joint probability density function of the basic random variables at time t. In general, the joint probability density function is unknown, and evaluating the convolution integral is a formidable task. Several practical approaches including first-order reliability method (FORM), SORM and Monte Carlo simulation are usually used. SORM available in the general-purpose reliability analysis software COMPASS by Orisamolu et al. [25,26] is used in the demonstration example. The theories of FORM, SORM, and Monte Carlo Simulation are well established and can be found in Ayyub and McCuen [27].

3.2. Time-dependent reliability

In the presence of degradation mechanisms, the ship hull ultimate strength $U(t)$ is a decreasing function of time, therefore, the probability of failure is also a function of time. By varying the time period t from zero to an expected service life, the decreasing values of ultimate strength $U(t)$ can be estimated. Furthermore, the instantaneous failure probability at any time t, defined by $P[U(t) < L(t)]$ without regard to survival of a vessel in the previous years can be obtained using Eq. (26).

Successive, yearly loading and decreasing values of yearly ship ultimate strength are however dependent events and must be accounted for in reliability estimation. This is accomplished by using time-dependent or progressive reliability estimates that are based on conditional probability theory. The hazard rate or failure function strategy is used in this study. The progressive or time-dependant reliability, $\gamma_p(t)$, of a degrading ship structure is given by

$$\gamma_p(t) = \exp\left(-\int_0^t \lambda(\tau)\,\mathrm{d}\tau\right), \tag{27}$$

where τ is the variable of integration, and $\lambda(t)$ is a conditional probability function called the hazard rate [28–31] and is defined by $\lambda(t)=$Prob[Failure between time t and $t+\mathrm{d}t$|no failure up to time t]. For continuous systems, the hazard rate is defined by Ang and Tang [34] as

$$h(t) = \frac{f(t)}{1 - F(t)}, \tag{28}$$

where $f(t)$ is the joint probability density function and $F(t)$ is the joint cumulative density function. For discrete space with one year increment, the hazard function becomes

$$h(t_i) = \frac{P_f(t_i)}{1 - \sum_{j=1}^{i-1} P_f(t_i - 1)}. \tag{29}$$

Substituting Eq. (29) into Eq. (27) gives the time-dependent reliability. The time-dependent failure probability is given by

$$P_{ft}(t) = 1 - \gamma_p(t), \tag{30}$$

where the subscript ft is for time-dependent failure probability. Eq. (30) is used to estimate the progressive or time-dependent reliability. It is emphasized that $P_{ft}(t) = 1 - \gamma_p(t)$ is not equivalent to $P[R(t) < L(t)]$, the latter being just an instantaneous failure at time, t, without regard to previous or future performance. This is a very important point that is lacking in much of the literature that is available.

4. Demonstration example

The principal dimensions of the hull and structural details used in the demonstration example are given in Table 1. It is assumed that the tanker experiences both fatigue and corrosion. Schematic diagrams of the vessel and its cross-sectional profile and dimensions are shown in Figs. 2 and 3, and Table 2. Furthermore, it is assumed that general corrosion of primary hull structure is prevalent after 5 years and that the corrosion grows at a constant rate. Also, it is assumed that cracking of major and minor structures in the midship is prevalent after 5 years and that the cracks grow according to corrosion-enhanced Paris law.

Short-term extreme wave conditions that result in the largest wave-induced bending moments among the various sea states that are encountered by the vessel are used in the yearly analyses. A significant wave height of 10 m is used to model the wave load and the vessel is assumed to operate at 12 knots. The ship is assumed to remain in this peak sea condition for 3 h. The long-term mean value of the still-water bending moment is calculated based on IACS formulae. For this example problem, the maximum still-water bending moments occur in sagging conditions, therefore, results for only this condition are presented. Probabilistic characteristics of the still-water bending moment and the wave-induced bending moment used in the analyses are presented in Table 3, and probabilistic characteristics of the modeling uncertainty factors are given in Table 4. Although, the buckling knock down factor is of high variability and depends on ship type or class and the location of a section, it was considered as a constant in this study.

Table 1
Principal dimensions of a tanker vessel

Item	Dimension (m)
Length (L)	220
Breadth (B)	38.1
Depth (D)	17.4
Draft (T)	13.5
Block coefficient	0.75

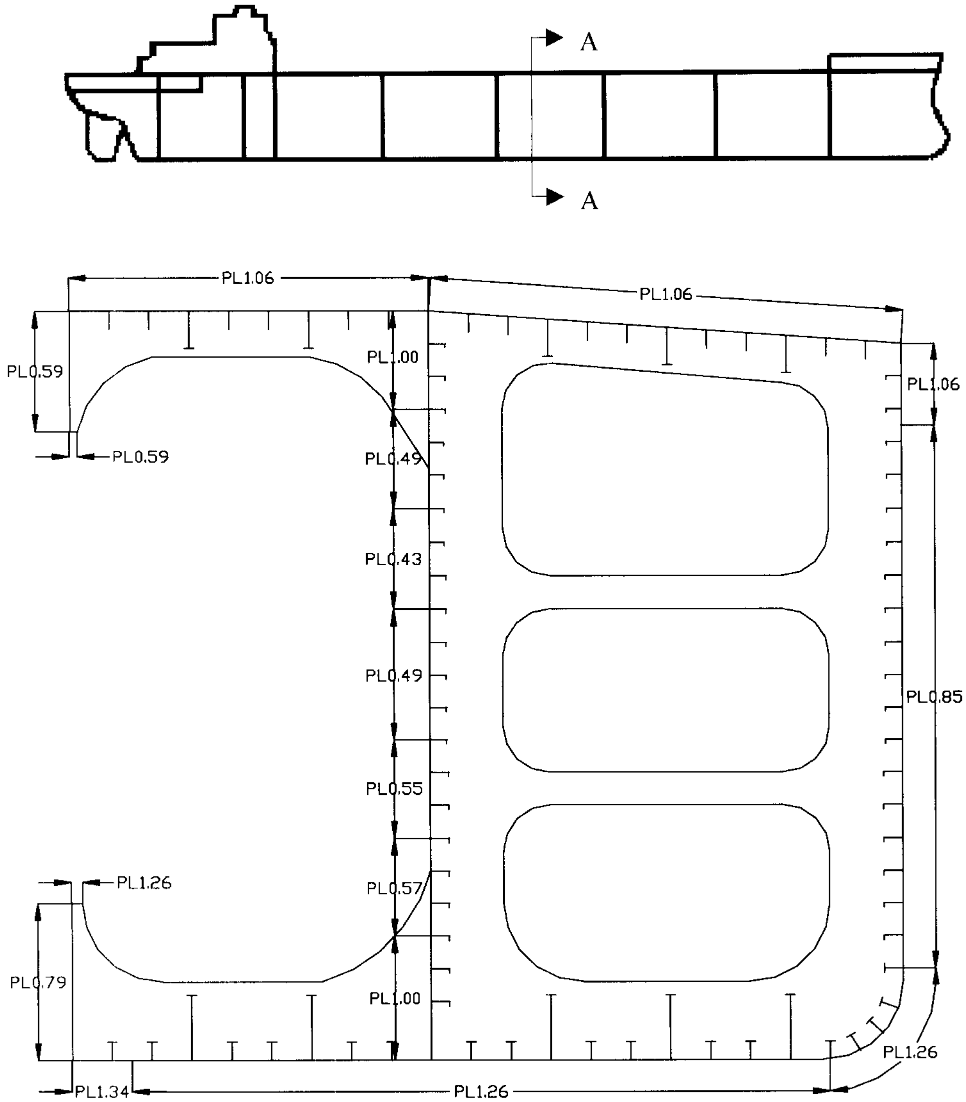

Fig. 2. Schematic diagram of tanker (Section A–A): dimensions of longitudinal plating (inches).

It is assumed that each and every member of the hull crosssection experiences thickness reduction due to general corrosion after 5 years and that there is no painting, steel renewal or corrosion repair. Typical corrosion growth rates for various members of the primary hull structure given in Table 5 are adapted from TSCF [32]. Probabilistic characteristics of the yearly corrosion rates for the different members are given in Table 6. The effect of spatial variability of the general corrosion is not considered by assuming the corrosion to be homogeneous (i.e., uniform) in its distribution for each member. It is assumed that cracking starts

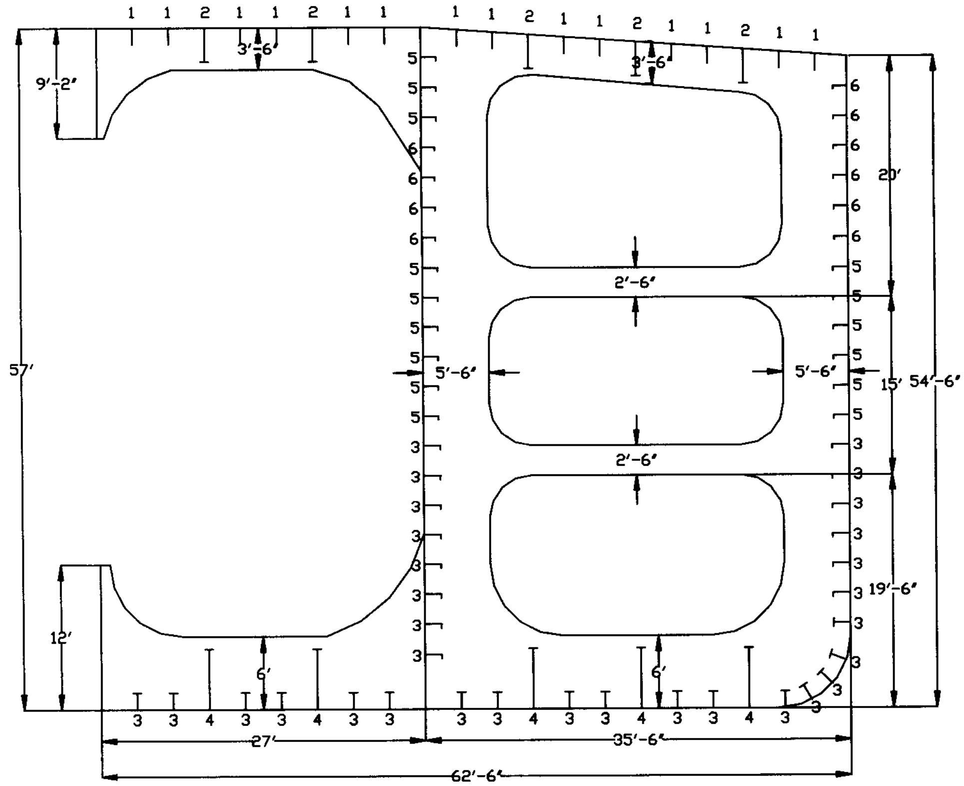

Fig. 3. Schematic diagram of tanker: dimensions of crosssection (feet and inches)/stiffener types.

Table 2
Stiffener dimensions

Stiffener dimensions (mm)		
Stiffener no.	Web	Flange
1	450 × 36	
2	1000 × 16	400 × 16
3	465 × 18	190.5 × 25.5
4	1220 × 16	350 × 25.5
5	370 × 16	100 × 16
6	297 × 11.5	100 × 16

after 5 years and the crack sizes are the same at all stiffeners and plating, although it is recognized that in practice, crack sizes vary with joints. Table 7 presents the crack growth parameters. Furthermore, it is assumed that there is no repair to fix the cracks.

Fig. 4 shows the normalized mean values of the hull section modulus without corrosion or cracks, with corrosion, with fatigue and with both degradation modes.

Table 3
Probabilistic characteristics of principal random variables

Random variable	Mean value	Coefficient of variation	Distribution type
Ultimate stress, σ_u	281 MPa	0.1	Lognormal
Knockdown factor, c	0.95		Fixed
Stillwater moment, M_{sw}	2053 MN m	0.4	Normal
Wave induced moment, M_w	3205 MN m	0.1	Extreme

Table 4
Probabilistic characterization of model uncertainty random variables [9]

Random variable	Distribution type	Mean	Coefficient of variation
X_u	Normal	1.0	0.15
X_{sw}	Normal	1.0	0.05
X_w	Normal	0.9	0.15
x_s	Normal	1.15	0.03

Table 5
Typical corrosion rates for tanker members [32]

Corrosion rates			
Location	Mean (mm/yr)	Min (mm/yr)	Max (mm/yr)
Deck plating	0.065	0.03	0.10
Deck longitudinals (web)	0.065	0.03	0.10
Side shell plating	0.030	0.03	0.03
Side shell plating longitudinals (web)	0.030	0.03	0.03
Bottom shell plating	0.170	0.03	0.30
Bottom shell longitudinals (web)	0.065	0.03	0.10
Longitudinal bulkhead plating	0.065	0.03	0.10
Longitudinal bulkhead longs. (web)	0.065	0.03	0.10

Table 6
Probabilistic characterization of random variables related to corrosion

Corrosion rates			
Location	Mean (mm/yr)	Coefficient of variation	Distribution type
Deck plating	0.065	0.5	Weibull
Deck longitudinals (web)	0.065	0.5	Weibull
Side shell plating	0.030	0.1	Weibull
Side shell plating longitudinals (web)	0.030	0.1	Weibull
Bottom shell plating	0.170	0.5	Weibull
Bottom shell longitudinals (web)	0.065	0.5	Weibull
Longitudinal bulkhead plating	0.065	0.5	Weibull
Longitudinal bulkhead longs. (web)	0.065	0.5	Weibull

Table 7
Probabilistic characterization of random variables related to cracks

Random variable	Mean	Coefficient of variation	Distribution type
A_0	1.0	0.1	Extreme
M	2.5	1.0	Fixed
C	1.16×10^{-9}	0.1	Lognormal
Y	1.0	1.0	Fixed

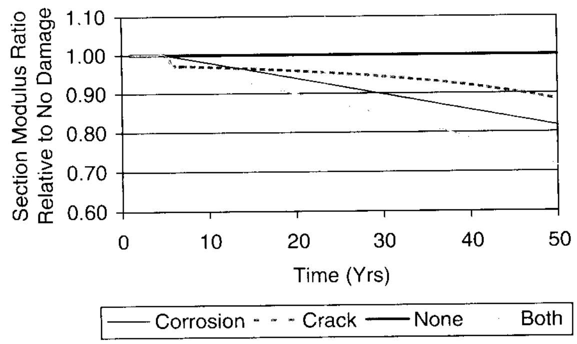

Fig. 4. Variation of mean value of ship section modulus with age.

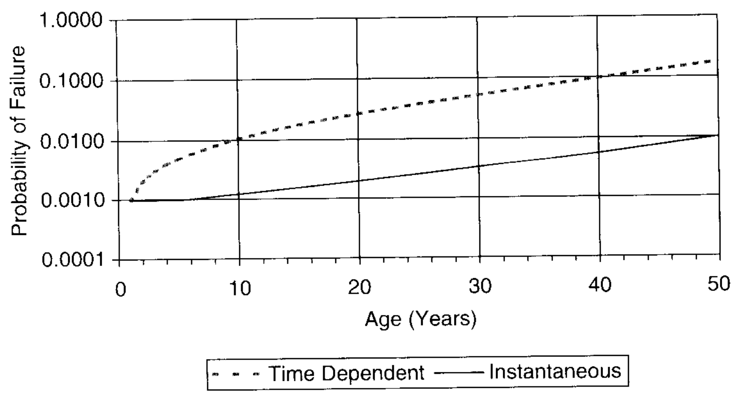

Fig. 5. Instantaneous and time-dependent probabilities of failure for a tanker with corrosion.

Plots of the instantaneous and time-dependent probabilities of failure and reliability indices of the primary hull structure with corrosion and with fatigue are shown in Figs. 5–10. The following general comments are applicable to the results. Instantaneous failure probabilities are always smaller than time-dependent failure probabilities, or conversely instantaneous reliability indices are always greater than time-dependent reliability indices, therefore, instantaneous failure probabilities (reliability indices) might not be given very reliable estimates of structural risk in the

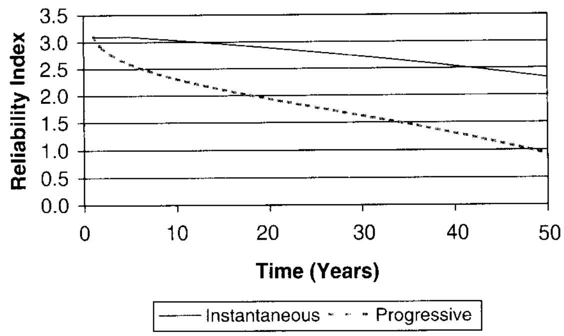

Fig. 6. Instantaneous and time-dependent reliability index for a tanker with corrosion.

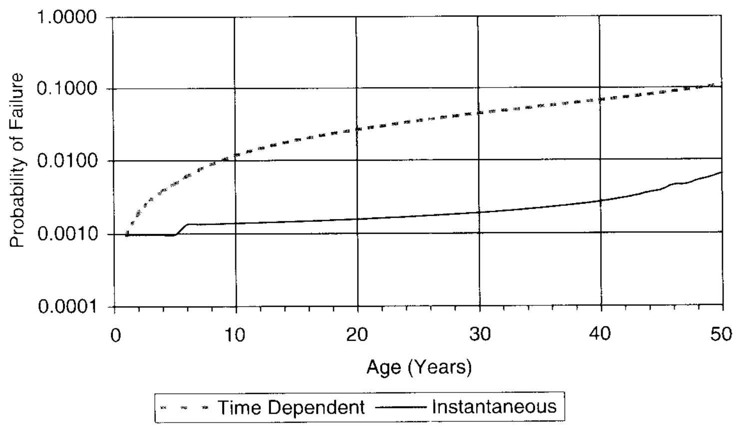

Fig. 7. Instantaneous and time-dependent probabilities of failure for a tanker with cracks.

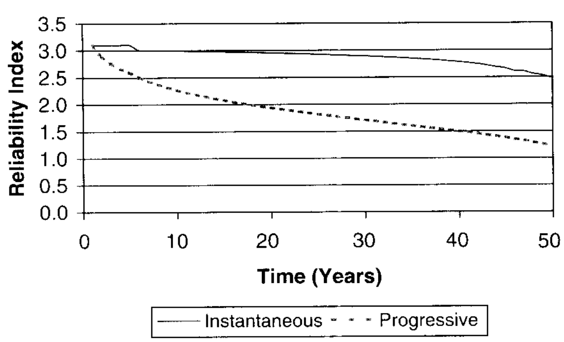

Fig. 8. Instantaneous and time-dependant reliability index for a tanker with cracks.

presence of degradation modes. A better measure of structural risk is the time-dependent probability of failure. The impact of the growth of structural degradation models with time is reflected in the increase value of instantaneous failure

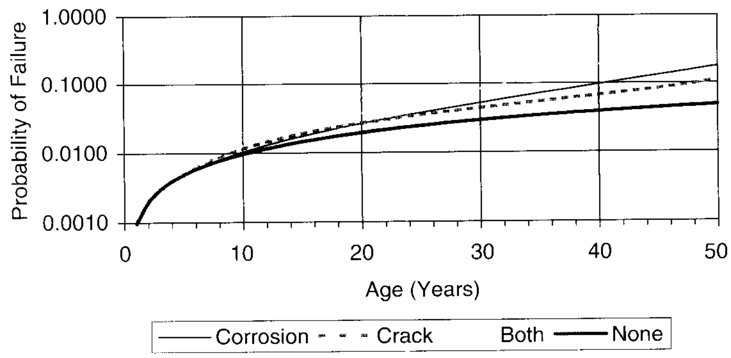

Fig. 9. Time-dependent probability of failure.

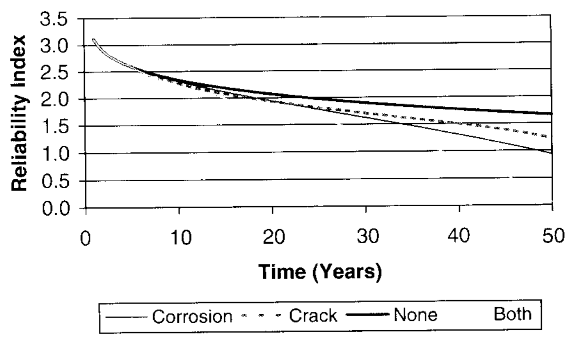

Fig. 10. Time-dependent reliability index.

probabilities and decrease section modulus with age. Combined effect of operation and degradation is accounted for in the estimate of time-dependent probabilities of failure. The retirement age of a vessel depends on the value of the target reliability and classification society rules. The selection of this value can reflect the gravity of failure consequences. Using a target reliability of 0.95, the corroding tanker vessel is this example, which has not been maintained will have to be retired after it has been in operation for 29 years. The values of the time-dependent reliabilities can be used to set maintenance and inspection dates based on targeted values. For example, based on a target reliability of 0.99, the corrosion in the vessel should be repaired by 10 years.

Sensitivities of the structural integrity of the vessel to probabilistic characteristics of the corrosion growth and corrosion-enhanced fatigue growth parameters have been investigated. The findings are presented in Figs. 11–16. It is seen that the failure probabilities (reliability indices) are not very sensitive to the probabilistic distribution of the corrosion growth rate parameters and corrosion-enhanced fatigue growth parameters. It is more sensitive to the mean value of corrosion-enhanced fatigue growth parameter. Therefore, more resources should be directed toward accurate calibration of the mean value of corrosion growth rates.

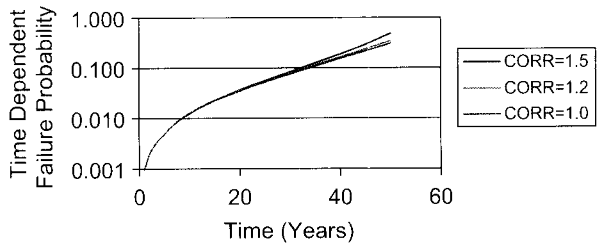

Fig. 11. Sensitivity of time-dependent probability of failure to the mean value of corrosion-enhanced fatigue growth parameter.

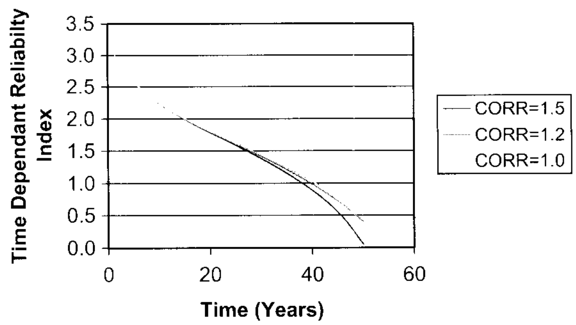

Fig. 12. Sensitivity of time-dependent reliability index to the mean value of corrosion-enhanced fatigue growth parameter.

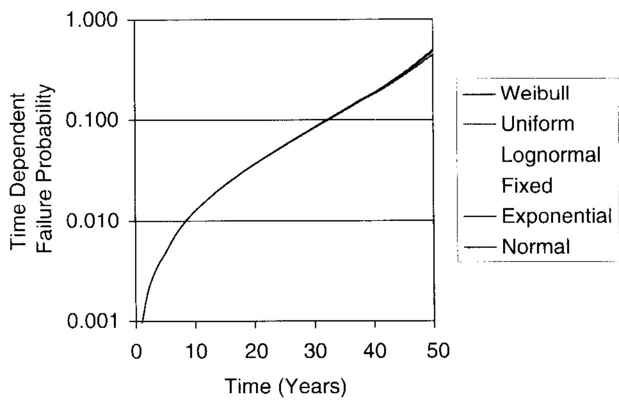

Fig. 13. Sensitivity of time-dependent probability of failure to the probabilistic characterization of corrosion-enhanced fatigue growth parameter.

5. Limitation of results

The following limitations apply to the results that have been presented: International Association of the Classification Societies (IACS) [33] has guidelines

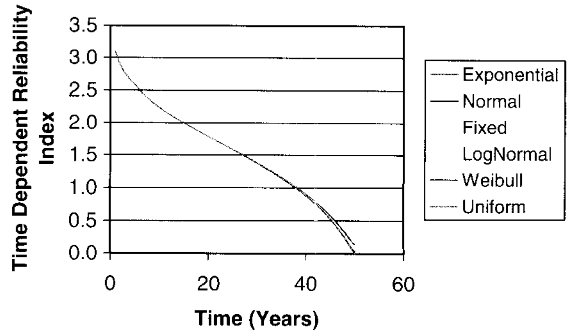

Fig. 14. Sensitivity of time-dependent reliability index to the probabilistic characterization of corrosion-enhanced fatigue growth parameter.

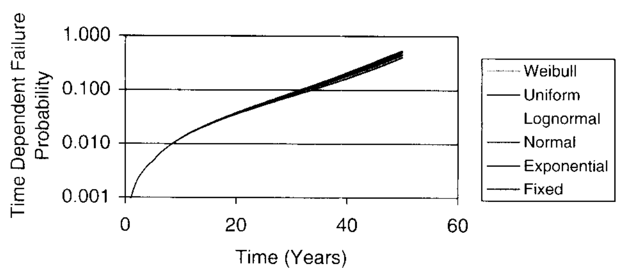

Fig. 15. Sensitivity of time-dependent probability of failure to the probability distribution of the corrosion growth parameter.

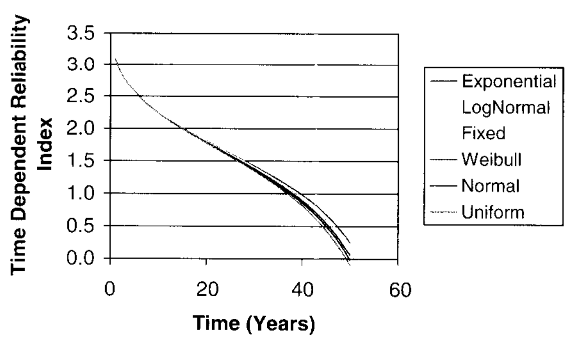

Fig. 16. Sensitivity of time-dependent reliability index to the probability distribution of corrosion growth parameter.

on minimal allowable corrosion margins for ship structural members. Operators of tankers are expected to renew those members once the allowable corrosion margins are reached. Renewal of structural members is not included in the analyses. Also, general corrosion does not operate independent of pitting and it is well known that cracks and corrosion usually exist simultaneously in vessels. The simultaneous effect of pitting and general corrosion is not considered in the studies. Therefore, the value of time-dependent failure probabilities that are estimated in this study could be non-conservative. Furthermore, the presence of pitting corrosion could lead to leaks resulting in environmental risk and this has not been considered in the presentation. The rate of corrosion growth is assumed to be invariant with time, and this might not be true in all locations and cases. The fidelity of the reliability results depends on the integrity of the structural model used for ultimate strength capacity. An analytical model is used in the demonstration example, however, numerical models such as the ISUM method might improve the quality of the result. The wave bending moment and the still-water bending moment used in the analysis are assumed to be invariant with time. This might not be true in all cases; extreme loading conditions are used in the analyses, therefore, it is expected that the time-dependent structural integrity results could be conservative.

6. Conclusions

A practical strategy for risk assessment of the ultimate strength capacity of an aging ship subject to structural degradations has been presented. Time-dependent random function models for corrosion growth, fatigue cracks and corrosion-enhanced fatigue cracks that weaken the capacity of a ship hull have been developed. The second-order reliability method (SORM) was used to calculate instantaneous reliability of the primary hull structure. Methodology for computing the time-dependent reliability of a degrading aging ship structure has been advanced. An example of a problem involving an aging tanker structure has been used for demonstration. Sensitivities of the aging structure reliability to statistical and probabilistic description of corrosion and fatigue crack parameters have been investigated. It is shown that, in general, the time-dependent reliability is always lower than instantaneous reliability and is a better estimate of the risk of operating an aging degrading vessel. Sensitivity studies on the example problem indicate that the time-dependent reliability is not very sensitive to probabilistic distribution description of corrosion growth and corrosion-enhanced fatigue growth parameters, it is more sensitive to the first moment of the corrosion-enhanced fatigue growth parameter.

References

[1] Bea RG, Cramer E, Schulte-Strauthaus R, Mayoss R, Gallion K, Ma K, Holzman R, Demsetz L. Ship's Maintenance Project. Conducted at University of California, Berkeley for US Coast Guard/ Ship Structure Committee (SSC), SSC-386, 1995.

[2] Soares CG, Garbatov Y. Reliability of maintained ship hull girders subjected to corrosion and fatigue. Struct Saf 1998;20:119–201.

[3] Atua KI. Reliability-based structural design of ship hull girders and stiffened panels. Dissertation, submitted to the Faculty of the Graduate School of the University of Maryland, College Park, in partial fulfillment of the requirements for the degree of Doctor of Philosophy, 1998.

[4] Atua KI, Ayyub BM. Development of LRFD rules for naval surface ship structures: reliability-based load and resistance factor design rules. Part I - Hull girder bending. US Navy, Naval Sea System Command, Washington, DC, 1996.
[5] Mansour A, Thayamballi. Probability-based ship design: loads and load combinations. SSC-373, Ship Structures Committee, NTIS # PB94-188208, Springfield, VA, 1994.
[6] Mansour AE, Wirsching PH, Lucket MD, Lin YH. Structural safety of ships. Proceedings of the Society of Naval Architects and Marine Engineers SNAME Meeting, Ottawa, Paper No. 3, 1997.
[7] Thayamballi AK, Chen YK, Chen HH. Deterministic and reliability based retrospective strength assessment of oceangoing vessels. Trans. SNAME 1987;95:159–87.
[8] Caldwell JB. Ultimate longitudinal strength. Trans. RINA, 1965.
[9] Mansour AE, Howen L. Probability-based ship structural safety analysis. J Ship Res 1994;38(4):329–39.
[10] Billingsley D. Hull girder response to extreme bending moments. In: Proceedings of the SNAME STAR Symposium, Coronado, CA, 1980.
[11] Ostapenko A. Strength of ship hull girders under moment, shear and torque. Proceedings of the SSC-SNAME Extreme Loads Response Symposium, Arlington, VA, 1981.
[12] Adamchak JC. An approximate method for estimating the collapse of a ship's hull in preliminary design. Proceedings of the SSC-SNAME Ship Structure Symposium, Arlington, VA, October 1984.
[13] Dow RS, Hugill RC, Clark JD, Smith CS. Evaluation of ultimate ship hull strength. Proceedings of the SSC-SNAME Extreme Loads Response Symposium, Arlington, VA, 1981.
[14] ABS. Guide for fatigue strength assessment of tankers. American Bureau of Shipping, June 1992.
[15] Paik JK. ALPS/ISUM: A computer program for non-linear analyses of large plated structures using the idealized structural unit method. Pusan National University, Pusan, 1993.
[16] Orisamolu IR, Luo X, Lichodzijewski M. Development of optimal strategies for inspection/monitoring/maintenance/repair and life extension. Canadian Department of National Defense Final Report, 1999, about 120pp.
[17] Orisamolu IR, Akpan UO, Brennan DB. Application of probabilistic corrosion models for reliability assessment of ship structural panels. Presented at the Eighth CF/CRAD Meeting on Naval Application of Materials Technology and Inter-naval Corrosion Conference, Halifax, NS, 1999.
[18] Orisamolu IR, Brennan DB, Akpan UO. Probabilistic modeling of corroded ship structural panels. Presented at the Eighth CF/CRAD Meeting on Naval Application of Materials Technology and Inter-naval Corrosion Conference, Halifax, NS, 1999.
[19] Paik JK, Kim SK, Lee SK. Probabilistic corrosion rate estimation model for longitudinal strength members of bulk carriers. Ocean Eng 1998;25(10):837–60.
[20] Hughes OF. Ship structural design: a rationally based computer-aided optimization approach. New York: Wiley-Interscience Publication, 1983.
[21] Orisamolu IR, Brennan DB, Akpan UO. Probabilistic residual strength assessment of damaged pipelines. Martec Technical Report, TR-98-07, 1999.
[22] Nitta A, Arai H, Magaino A. Basis of IACS unified longitudinal strength standard. Marine Struct 1992;5:1–21.
[23] Jensen JJ, Petersen PT. Wave induced bending moments in ships – a quadratic theory. Trans. RINA, Supplementary Paper 1979;121:151–65.
[24] Loukakis TA, Chryssostomidis C. Seakeeping Series for Cruiser Ships. Trans. SNAME 1975;83.
[25] Orisamolu IR, et al. Pilot studies for structural risk assessment program (STRAP). Technical Report submitted to the Defence Research Establishment Atlantic (DREA), Halifax, NS, 1993.
[26] Orisamolu IR, Liu Q, Chernuka MW. Development of computational algorithms for probabilistic fatigue and fracture reliability. Martec Technical Report No. TR-93-07, July 1993.
[27] Ayyub BM, McCuen RH. Probability, statistics, and reliability for engineers. CRC Press, Florida, 1997.
[28] Akpan UO, Luo X. Probabilistic analysis of solid rocket motors. Martec Technical Report TR-00-11, 2000.
[29] Ellingwood BR, Mori Y. Probabilistic methods for condition assessment and life prediction of concrete structures in nuclear plants. Nucl Eng Design 1993;142:155–66.

[30] Heller RA, Thanjitham S. A survey of probabilistic service life prediction models for structures. In: Spanos PD, Wu YT, editors. IUTAM symposium on probabilistic structural mechanics. NY: Springer, 1993. p. 237–67.

[31] Soares CG, Ivanov LD. Time-dependent reliability of the primary ship structure. Reliab Eng Syst Saf 1989;28:59–71.

[32] TSCF (Tanker Structure Cooperative Forum). Guidance manual for tanker structures. Issued by Tanker Structure Co-operative Forum in association with International Association of Classification Societies, Witherby & Co. Ltd., 1997.

[33] IACS (International Association of Classification Societies). Bulk carriers—Guidelines for Surveys, Assessment and Repair of Hull Structure, 1994.

[34] Ang AA-H, Tang WH. Probability Concepts in Engineering Planning and Design, Volume II: Decision, Risk and Reliability, John Wiley and Sons, 1984.

[35] Dobson WG, Brodrick RF, Wheaton JW, Giannotti J, Stambaugh KA. Fatigue Considerations in View of Measured Load Spectra, SSC-315, 1983.

[36] Manning SD, Yang JN. Advanced Durability Analysis, Volume II-Analytical Predictions, Test Results and Analytical Correlations, Air Force Wright Aeronautical Laboratories, AFWAL-TR-3017, 1989.